(2)

NSWC TR 88-226

AD-A241 549

BUBBLE DYNAMICS CALCULATIONS USING THE DYSMAS/E FINITE DIFFERENCE CODE

BY STEPHEN A. WILKERSON (NSWC)
DR. HANS SCHITTKE (IABG)

FOR NAVAL SURFACE WARFARE CENTER
RESEARCH AND TECHNOLOGY DEPARTMENT

JULY 1988

91-13406

NAVAL SURFACE WARFARE CENTER

Dahlgren, Virginia 22448-5000 • Silver Spring, Maryland 20903-5000

Original contains color plates: All DTIC reproductions will be in black and white

REPORT DOCUMENTATION PAGE

1a. REPORT SECURITY CLASSIFICATION UNCLASSIFIED	1b. RESTRICTIVE MARKINGS
2a. SECURITY CLASSIFICATION AUTHORITY	3. DISTRIBUTION/AVAILABILITY OF REPORT Approved for public release; distribution is unlimited.
2b. DECLASSIFICATION/DOWNGRADING SCHEDULE	
4. PERFORMING ORGANIZATION REPORT NUMBER(S) NSWC TR 88-226	5. MONITORING ORGANIZATION REPORT NUMBER(S)
6a. NAME OF PERFORMING ORGANIZATION Naval Surface Warfare Center 6b. OFFICE SYMBOL (If applicable) R14	7a. NAME OF MONITORING ORGANIZATION
6c. ADDRESS (City, State, and ZIP Code) White Oak Laboratory 10901 New Hampshire Avenue Silver Spring, MD 20903-5000	7b. ADDRESS (City, State, and ZIP Code)
8a. NAME OF FUNDING/SPONSORING ORGANIZATION Office of Naval Technology 8b. OFFICE SYMBOL (If applicable) ONT-23	9. PROCUREMENT INSTRUMENT IDENTIFICATION NUMBER
8c. ADDRESS (City, State, and ZIP Code) 800 North Quincy Street Arlington, VA 22217-5000	10. SOURCE OF FUNDING NOS. PROGRAM ELEMENT NO. 62314N PROJECT NO. RJ14W27 TASK NO. WORK UNIT NO.

11. TITLE (Include Security Classification)
Bubble Dynamics Calculations Using the DYSMAS/E Finite Difference Code

12. PERSONAL AUTHOR(S)
Wilkerson, Stephen A. (NSWC) and Schittke, Dr. Hans (IABG)

13a. TYPE OF REPORT	13b. TIME COVERED	14. DATE OF REPORT (Yr., Mo., Day)	15. PAGE COUNT
Final	FROM 1/87 TO 2/87	1988, July	24

16. SUPPLEMENTARY NOTATION

17 COSATI CODES		
FIELD	GROUP	SUB. GR.
19	09	

18. SUBJECT TERMS (Continue on reverse if necessary and identify by block number)
bubble dynamics
bubble collapse
DYSMAS/E code
detonation

19. ABSTRACT (Continue on reverse if necessary and identify by block number)

A method of calculating underwater bubble collapse using the DYSMAS/E code is presented. The effects on bubble growth and collapse of a nearby rigid boundary and the free surface are included in the analysis. The solution methodology is described, and the advantages and disadvantages of compressible flow theory are compared to incompressible flow theory. The approach is shown to give reasonable results in comparison to observed explosion bubble behavior. This report also contains a preliminary look at the formation of a bubble jet.

20. DISTRIBUTION/AVAILABILITY OF ABSTRACT	21. ABSTRACT SECURITY CLASSIFICATION
___ UNCLASSIFIED/UNLIMITED X SAME AS RPT ___ DTIC USERS	UNCLASSIFIED

22a. NAME OF RESPONSIBLE INDIVIDUAL	22b. TELEPHONE NUMBER (Include Area Code)	22c. OFFICE SYMBOL
Kenneth C. Kiddy	(202) 394-2888	R14

FOREWORD

This work was sponsored by the Explosives and Undersea Warheads Block Program at the Naval Surface Warfare Center (NSWC), Silver Spring, Maryland, and the German Federal Ministry of Defense in Bonn, West Germany. The study represents a cooperative, 1-month effort which was conducted at the Industrieanlagen-Betriebsgesellschaft (IABG) Company in Munich. The IABG cooperation was established jointly in 1961 by the Federal Ministry of Defense and the German aerospace industry to provide technical support in test and evaluation for the Federal Republic of Germany. The purpose of this study was the investigation of underwater explosion bubble collapse with the German-developed code DYSMAS/E. The preliminary results from this study show that the DYSMAS/E code represents a significant contribution to analytical efforts in modeling underwater explosion phenomena. The authors gratefully acknowledge the help and support of Mr. Pfrang of IABG and Mr. Farley of NSWC whose continued support made this study possible.

Approved by:

WILLIAM H. BOHLI, Head
Energetic Materials Division

CONTENTS

ILLUSTRATIONS

ILLUSTRATIONS (Cont.)

SECTION 1

BACKGROUND

The Dynamic System Mechanics Advanced Simulation (DYSMAS) family of codes was developed by a West German firm Industrieanlagen-Betriebsgesellschaft (IABG). IABG was established jointly in 1961 by the Federal Ministry of Defense and the German aerospace industry. The firm's primary purpose was to provide technical support for the Ministry of Defense and aerospace industry in the area of advanced test and evaluation. Within the scope of IABG's responsibility, it was necessary to develop state-of-the-art analytical capabilities to supplement their expensive experimental work. Therefore, the DYSMAS family of codes was developed. The DYSMAS family of codes consists of a Lagrangian finite element code for structural analysis, design and optimization, an Eulerian finite difference code for analysis of fluid flow problems, and a coupled code which combines the two capabilities to handle fluid structure interaction problems. Each code incorporates features to handle the sophisticated analysis of current high-tech military and aerospace problems. For example, the DYSMAS Lagrangian code, DYSMAS/L, is capable of geometric and material nonlinearities as well as incorporating currently acceptable methodologies for material failure criteria based on strain, strain rate, and maximum effective stress. Additionally, the Eulerian code, DYSMAS/E, uses advanced constitutive relations for stress and strain, and it has been shown to give good results for the solution of difficult problems such as shaped charge analysis and design and underwater explosive detonations. During the course of the DYSMAS family of codes' development, numerous improvements have been and continue to be incorporated into the underlying theory behind the coding.

The focus of the current effort is the adaptability of the DYSMAS/E code for the study of underwater explosion bubble collapse. Prior analysis on underwater explosions with DYSMAS/E concentrated on the propagation of the explosion's shock wave in water and the interaction of the shock wave on nearby structural bodies. Some of the analysis performed using DYSMAS/E included the levels of structural response from a nearby underwater explosion on a ship or submarine, the associated shock wave loading, and the response of on-board equipment. However, most of these phenomena are considered early time events. More recently the applicability of the DYSMAS/E code for later time studies, such as bubble pulsation and collapse, was investigated. This work offers a limited discussion of the feasibility of the DYSMAS/E code's use for the study of underwater explosion bubble dynamics.

To highlight the diverse applicability of the current version of DYSMAS/E's formulation, a brief overview of the code's theoretical background is presented. The formulation of the DYSMAS/E code was based on an existing one dimensional finite difference code. The code employs the basic conservation of momentum, mass, and energy laws. The original one-dimensional model was extended to include two-dimensional cylindrical coordinate systems and two- and three-dimensional cartesian coordinate systems. The present DYSMAS/E finite difference code is still undergoing development. The code makes use of state-of-the-art discretization,

material models, equation of state formulations, and failure criteria. The present version of DYSMAS/E utilizes the Fluid-In-Cell (FLIC) finite difference method of Gentry, Martin, and Daly.[1]

The material model uses an elastic-plastic strength formulation with a linear-elastic constitutive relation for isotropic materials and a Von Mises yield criterion which takes into account the effects of strain, strain-rate, temperature, and pressure. Further, the code includes several burn models including constant velocity burn, the C-J volume burn, burn to detonation, and Forest Fire burn.[2-4] The code contains specific models for water, including cavitation affects; air, accounting for high energy dissociation and ionization; compacting soils; as well as an extensive list of high explosives. Among the equation of state models is the Jones Wilkins Lee (JWL) equation of state for explosives. In all, the code has an internal data bank of about 60 materials.

The failure criteria that can be used in DYSMAS/E provide for failure due to exceeding the maximum allowable distention of a material, the maximum effective stress, the maximum effective strain, or the hydrodynamic pressure. These criteria account for strain rate, temperature, and load state. After failure, the code simulates failure propagation in a material cell by introducing a small failed region which can grow according to an assumed load-dependent rate law. In this model a fully failed material will support no tensile load. However, recompression of a failed material is possible.

The DYSMAS/E code offers a variety of options for the advanced study of underwater explosion bubble dynamics. The methodologies include a number of equations of state for a variety of materials and explosives, sophisticated constitutive relations, and state-of-the-art material failure criteria. Therefore, DYSMAS/E allows a comprehensive treatment of the various factors influencing the expansion and collapse of explosion bubbles.

SECTION 2

PROBLEM DEFINITION

The purpose of this study was to explore the applicability of the DYSMAS/E code for the analysis of underwater explosion bubble collapse. In particular, DYSMAS/E's ability to predict the formation of a bubble jet toward a rigid boundary during the bubble's collapse phase was of primary importance. The problem chosen for analysis was that of a small explosive charge (1.4 grams of TNT) situated between a free surface and a rigid flat plate such that the bubble should collapse onto the rigid flat plate during its collapse phase. The location of the charge was approximately three-fourths of the expected maximum radius from the plate. At this location, a bubble jet was expected to form and impact on the rigid boundary near the end of the first bubble period. Figure 1 shows the geometry being studied. Selection of this configuration permits the problem to be easily duplicated experimentally.

The DYSMAS/E code offers a variety of detonation models including a fully exploded model, a C-J constant volume burn model, the burn-to-detonation model by Mader, the initiation and growth model by Lee and Tarver, and the Forest Fire model by Mader. In the interest of simplicity, a fully exploded model was chosen for the TNT explosive. In this model the original volume of TNT was converted to a high-pressure, high-temperature gas, thus providing the initial conditions for the dynamic expansion and contraction of the explosion products. The problem under consideration is axisymmetric, and a cylindrical coordinate system is used.

To take full advantage of DYSMAS/E rezoning features, an initial grid of 40 by 40 cells was used. Since the change in each cell must be calculated during a cycle and the shock wave can only propagate one cell per cycle, it would be inefficient to include a large grid initially. Therefore, use of a small grid reduces the computation time required for each cycle, and the rezoning feature can be used when required to expand the grid for the outward propagation of the explosion's shock wave. DYSMAS/E rezoning can be performed using an integer factor. For example, a factor of 2 along a coordinate axis would combine the information of two cells into one along that axis. Figure 2 shows the initial 40 by 40 grid and the location of the TNT cells within the grid. It was initially important to choose a sufficient number of cells being occupied by the TNT gaseous products and a sufficient number of fluid cells. Having sufficient cells occupied by the TNT gaseous products allows the detailed examination of the bubble jetting phenomena. An insufficient number of TNT gas cells would obscure the resolution, details, and accuracy of the analysis. Furthermore, the initial grid size and proportions become important when a rezoning is performed. This rezoning must be done in a way that preserves the initial grid's ratio of fluid cells to TNT gas cells. If this is not done correctly, the total number of cells required at each rezone will grow too rapidly, thus increasing the computation time, or the exclusion of sufficient cells for the TNT gas products will result in a degradation of computational accuracy. This balancing act of rezoning proportions requires a fair amount of user experience. To gain experience, several grid configurations in a one-dimensional

system, as well as several configurations in a two-dimensional system, were experimented with before choosing the final initial grid given in Figure 2. The importance of consistent rezoning procedures is due to the code's time dependence on shock wave speed. As the initial shock wave propagates outward, roughly at the speed of sound in water, the explosive gases continue to expand outward dropping the internal pressure of the TNT's gas products. This drop in gas pressure results in a decreasing outward momentum which is clearly time dependent. When the shock wave reaches the outer fluid cells, the analysis must be stopped and a rezoning must be performed before the analysis can continue. If at that time the bubble's gases have not expanded sufficiently, the total ratio of TNT to fluid cells will not be preserved after rezoning. This, in turn, will become a worsening problem with each additional rezone and a real problem throughout the analysis.

After the initial choice of grid sizes, the problem was rezoned four additional times. The final grid was utilized until the bubble jet formed and impacted on the rigid boundary. One additional rezoning would have increased the accuracy near the end of the collapse phase of the bubble period. However, the results obtained up to that point were sufficient for the purpose of this analysis, and no final rezoning was performed. The rezoning procedures in DYSMAS/E were very efficient, and the total rezoning process became so routine that a 5 to 10 minute operator time delay per rezone was all that was required before continuing the analysis. A plot showing the rezoning process and the amount of time in terms of computation cycles is shown in Figure 3. The first grid was a 40 by 40 grid of cells with the explosive located in the center of the grid along the line of symmetry. When the shock wave reached the outer cells along the line of symmetry, the analysis was stopped and a restart file was written. At that point the explosive gases, or explosion bubble, had expanded to about twice its original size. Therefore, a rezone factor of 2 in each direction would result in the combination of the current information from 4 cells into one cell. The overall result of this rezone is the preservation of initial bubble-to-cell ratio. Simply, the bubble was still being tracked by the same amount of cells as with the original grid. Consequently, this preserved the same level of accuracy for the bubble in the analysis. However, after the shock wave reached the line of symmetry in the second grid and a restart file was written, the bubble had not grown to twice its original size. Therefore, to preserve the equivalent level of discretization for the bubble, a finer mesh was required and a smaller rezone factor was used in that rezone. This resulted in a mesh of 60 by 80 cells which was roughly twice the actual size of the previous mesh. This type of philosophy was used throughout the rezoning process shown in Figure 3. In summary, the first and second choice of grids resulted in a larger number of cells being needed in the third and fourth rezoning. However, after the fourth rezoning, the bubble was sufficient in size so that the final rezoning was the last required. The final configuration consisted of a 60 by 65 grid with gradually expanding cells along the x and y axes which extended 3 meters high and 10 meters radially. The reason for the large final grid was to limit the influence of a reflected shock wave from a boundary. The exclusion of surrounding boundary constraints allowed the influence of the flat plate on bubble collapse to be studied more accurately.

SECTION 3

RESULTS

The results showed that the interaction of the bubble with the flat plate and the bubble's proximity to the free surface extended the bubble's period slightly, which was expected. When compared with empirical rules, the DYSMAS/E's predicted bubble period was 10 to 15 percent longer than an equivalent, free-field detonation which seemed reasonable. A number of plots were made throughout the analysis showing the behavior of the bubble and surrounding fluid. Several notable plots are shown (Figures 4 through 10) which duplicate expected bubble behavior during its growth and collapse in the proximity of a rigid boundary and near a free surface. Initially, the gaseous products from the explosive detonation become nearly spherical. The initial tin can shaped charge used in this analysis became nearly spherical after only 15 cycles, 1.024E-6 seconds, into the analysis. A velocity plot showing the outward movement of gaseous products and the beginning of the formation of the now nearly spherical shock wave is shown in Figure 4. In Figure 5 the outer circle, highlighted by the velocity vectors, is the shock wave in the fluid, and the darker inner circle shows the expanding bubble gases. As indicated, this velocity distribution is representative of expected shock wave formation and early time bubble growth and is very early in the analysis (5.315E-6 seconds). One additional velocity distribution is given in Figure 6. Figure 6 shows the rebounding shock wave from the rigid boundary which is seen propagating outward behind the initial shock wave. The dark inner velocity vectors show the near spherical expansion of the bubble's explosive gases.

To show the phenomena of bubble jetting as well as the magnitude of the bubble jet strength, several momentum distribution plots are presented. These plots indicate the magnitude of each cell's momentum relative to the other cells. In other words, higher momentum cells will be highlighted by larger vectors which can be seen as darkened areas on the plots. These larger momentum vectors become of interest in estimating the magnitude of the force being exerted on the rigid boundary by the bubble jet. Additionally the bubble's boundary can be estimated by recalling that momentum is the product of mass and velocity for each cell. Since the TNT gaseous products are of a very low density and the plot is scaled in accordance with the highest momentum, areas occupied by the TNT gas bubble are shown with little or no momentum. These areas are surrounded by high momentum fluid vectors and can be identified on the figures. Figure 7 shows a momentum distribution near maximum bubble expansion. The outward bubble expansion is highlighted by a dark ring of momentum vectors. Further, the interaction with the free surface can also be seen by the disoriented mix of momentum vectors extending from the upper portion of the bubble's surface to the free surface of the water. Figure 8 shows the initial contraction of the bubble and the beginning of the formation of a bubble jet near the top of the bubble surface. Finally, Figure 9 shows definite formation of a bubble jet, and Figure 10 shows the jet impacting on the rigid boundary. The results show conclusively that a bubble jet will form and impact on the rigid boundary under the initial

conditions imposed by this study. Further, the results indicate that the momentum in the area of the bubble's jet could be significant in deforming a nonrigid boundary. Finally, a number of color figures (Figures 11 through 18) track the expansion of the original explosive shock wave and the eventual expansion of the gaseous products of the bubble. The shock wave, shown in a lighter blue, expands in a near radial shape (Figure 11) until it reaches the nearly rigid boundary and the water's free surface and rebounds. The rebounding shock wave, also highlighted in a light blue, can be clearly seen in Figures 12 through 14. Figure 15 shows the continuing propagation of the original shock wave, the various rebounding shock waves, and begins tracking the expansion of the explosive's bubble, shown in red. Figures through 18 show the expansion of the bubble through its maximum. The bubble, highlighted as red boxes, is actually a near spherical shape at its maximum. However, the plotting routines in DYSMAS/E assign cells color in accordance with the dominant material. In other words, a cell with 40 percent gas and 60 percent water would be seen as blue, the color assigned for water, without indication of where the actual bubble boundary crossed the cell. Although the analysis considers where these boundaries are, the plotting does not; this is the reason for the boxy nature of the bubble's shape in the plots shown in Figures 11 through 18.

SECTION 4

CONCLUSION

The DYSMAS/E code represents a major contribution to the field of computational fluid dynamics and offers the opportunity to study complex physical phenomenon in detail. The code is easy to use, well written, and offers an abundance of features. The present study offers only limited results. However, the results presented indicate that the code is easily adapted for specific underwater applications. In particular, the code is well suited for the study of shock wave propagation as well as the study of underwater explosion bubble collapse.

The DYSMAS/E code offers a number of advantages over an incompressible, irrotational flow theory approach in analyzing an underwater explosion bubble collapse. The code methodology avoids the problems that occur in incompressible theory when the bubble jet penetrates the opposite surface of the bubble. Additionally, the effects of the energy loss after the bubble minimum are also partially accounted for in DYSMAS/E. DYSMAS/E will also allow the consideration of a deformable boundary. Incompressible theory currently does not address these complex phenomena which occur near the bubble minimum. The one negative aspect of DYSMAS/E is that the code is very computationally intensive and requires a large amount of computer time.

In conclusion, DYSMAS/E offers the opportunity to study particular cases of bubble jet collapse in detail, but is not well suited for parametric studies of bubble collapse. Such studies are better suited for incompressible flow theory, where multiple parameters can be studied, prior to bubble jet penetration, in a fraction of the computational time required by DYSMAS/E. However, DYSMAS/E offers the opportunity to study particular cases of bubble collapse with far more detail and information than an incompressible flow analysis. Furthermore, using the entire DYSMAS family of codes would enable the accurate study of target-bubble interaction and the possible inclusion of the bubble's damaging potential.

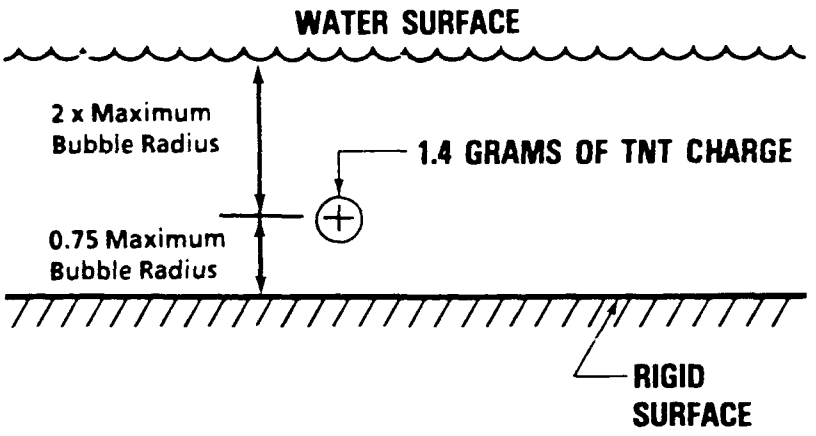

FIGURE 1. SHOT GEOMETRY

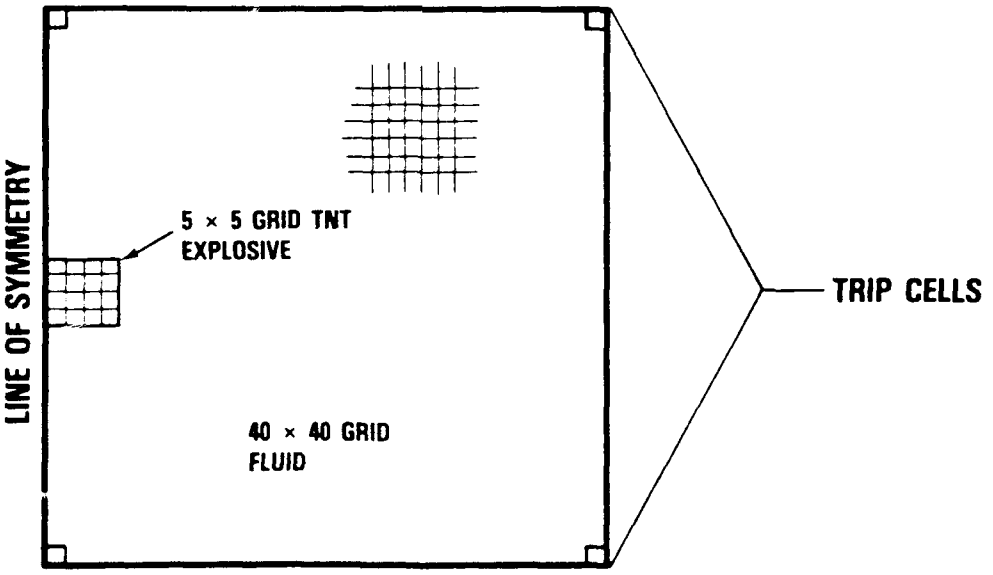

FIGURE 2. INITIAL CONDITITIONS

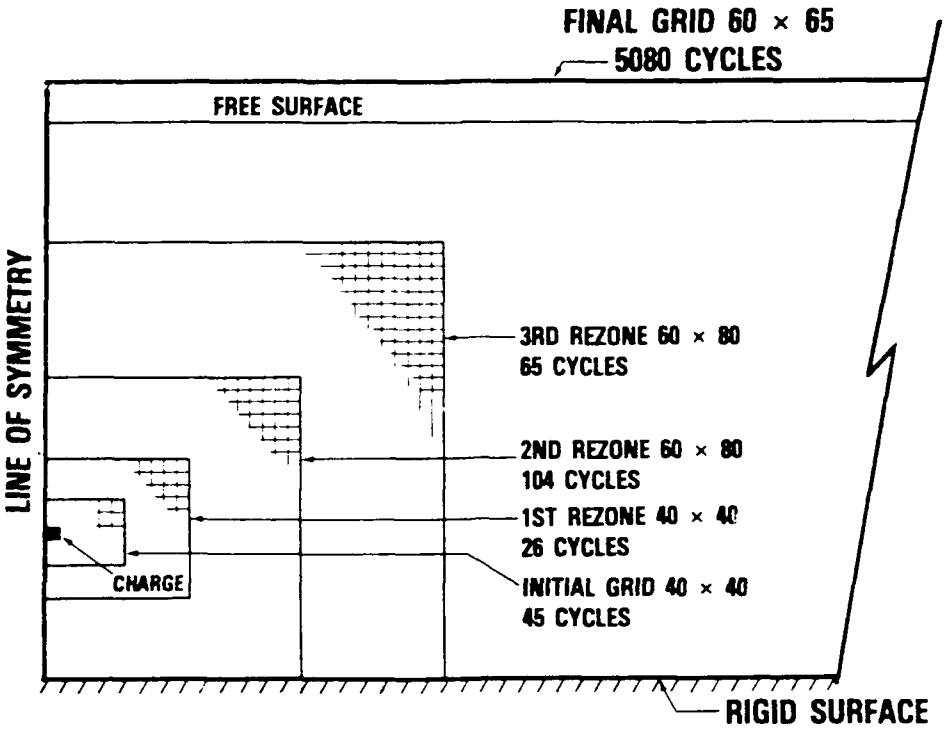

FIGURE 3. REZONING PLAN

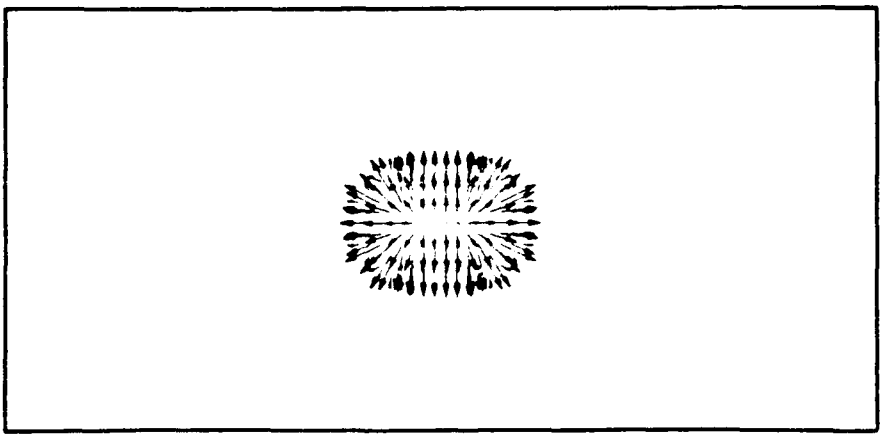

FIGURE 4. VELOCITY DISTRIBUTION (CYCLE 15, 1.024×10^{-6} SEC)

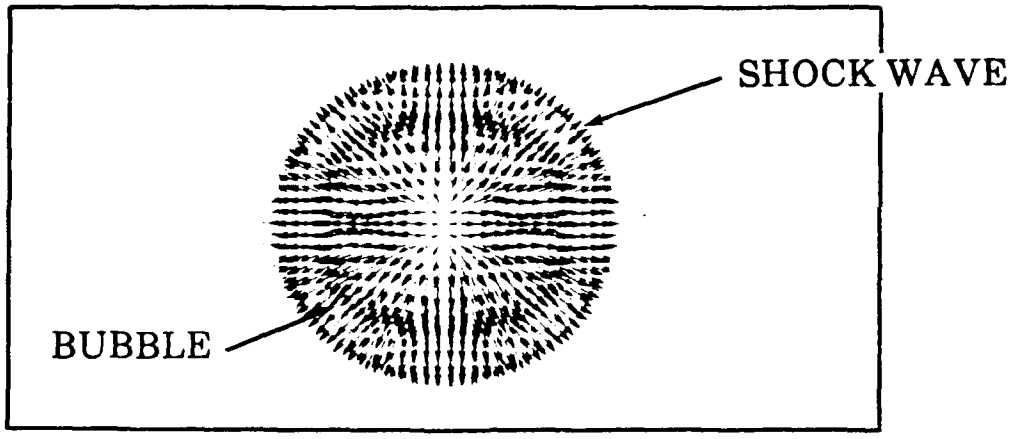

FIGURE 5. VELOCITY DISTRIBUTION (CYCLE 45, 5.315 x 10^{-6} SEC)

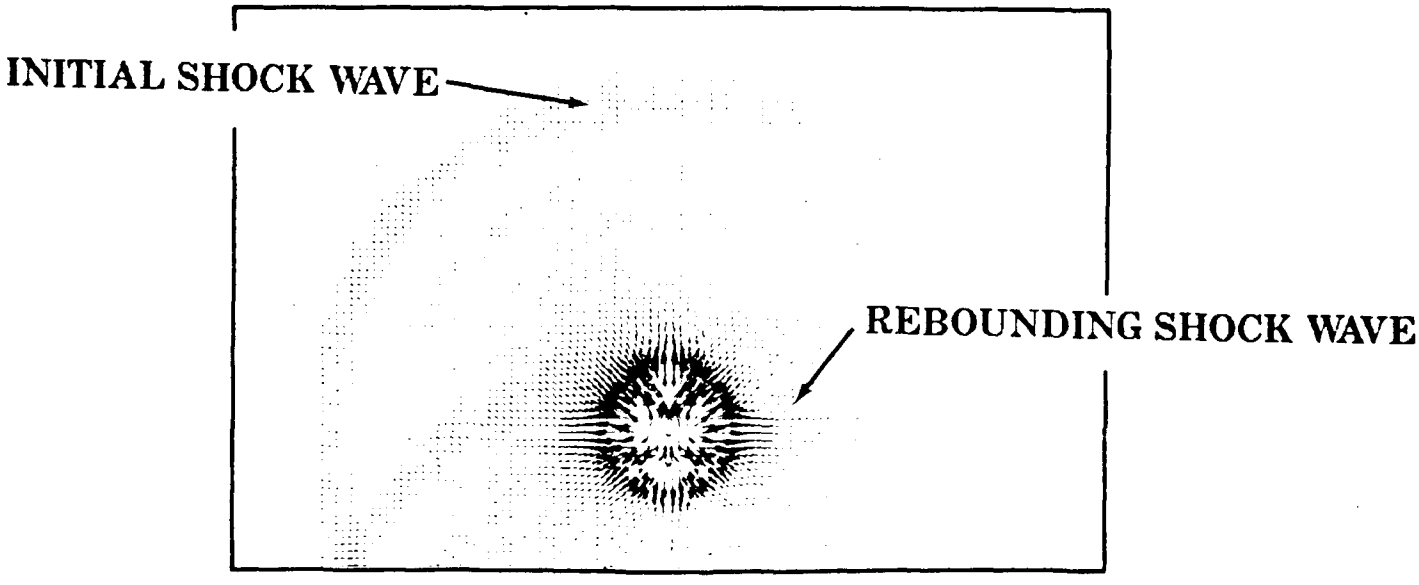

FIGURE 6. VELOCITY DISTRIBUTION (SECOND REZONE, CYCLE 104, 1.657 x 10^{-4} SEC)

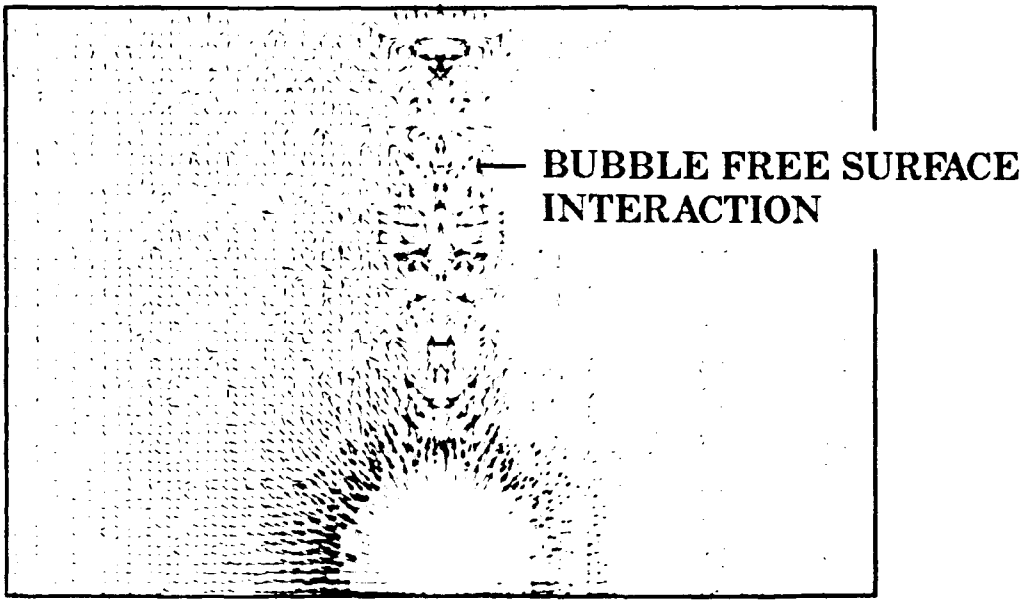

FIGURE 7. MOMENTUM DISTRIBUTION (FINAL GRID, CYCLE 1400, 1.008×10^{-2} SEC)

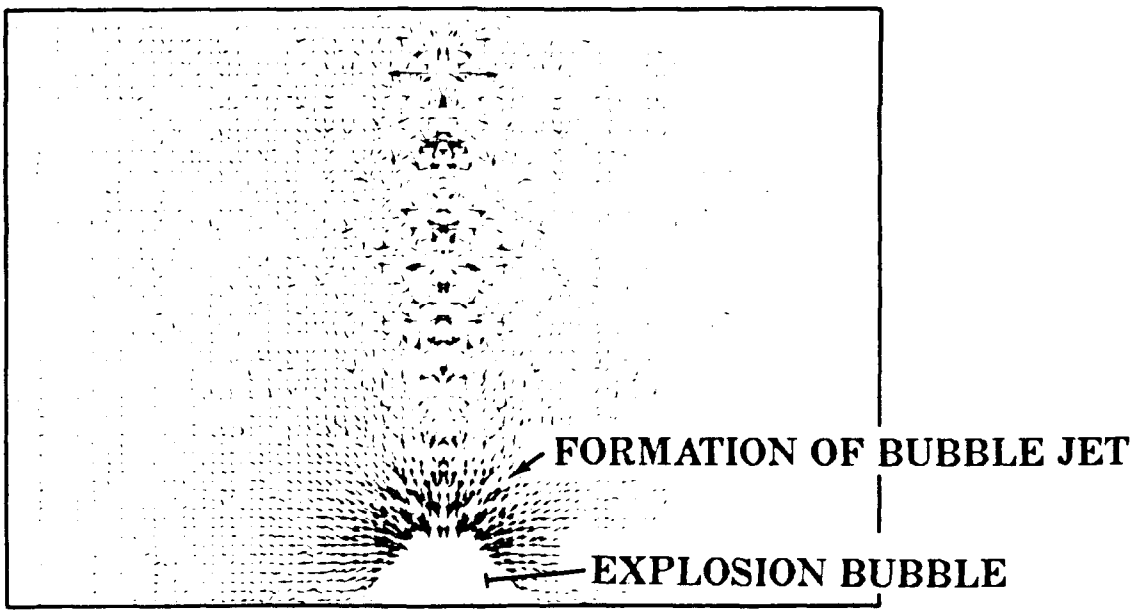

FIGURE 8. MOMENTUM DISTRIBUTION (FINAL GRID, CYCLE 3800, 2.685×10^{-2} SEC)

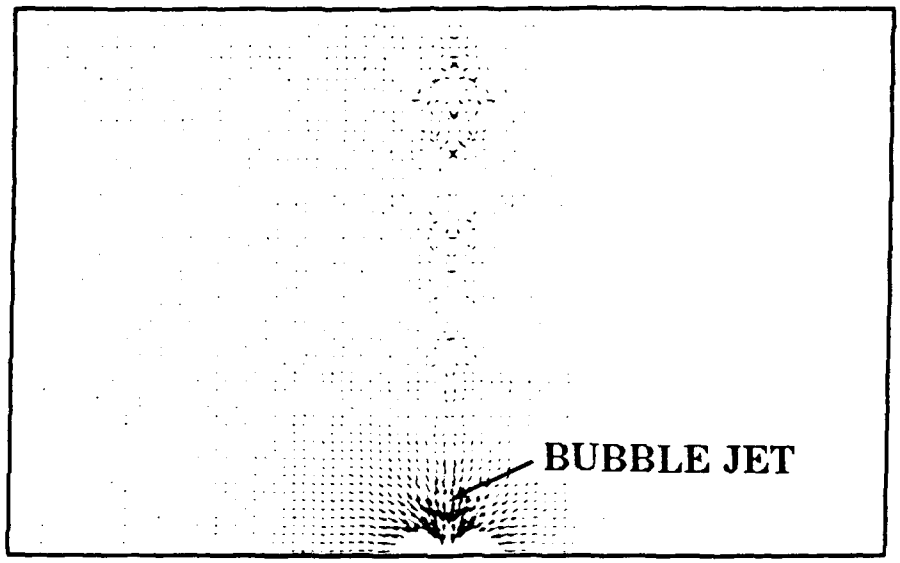

FIGURE 9. MOMENTUM DISTRIBUTION (FINAL GRID, CYCLE 4840, 3.408×10^{-2} SEC)

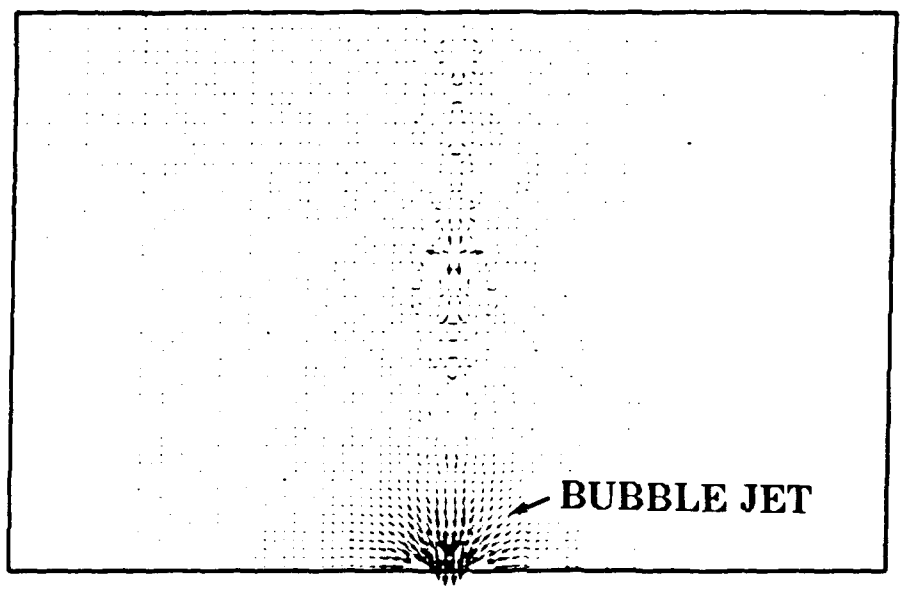

FIGURE 10. MOMENTUM DISTRIBUTION (FINAL GRID, CYCLE 5080, 3.573×10^{-2} SEC)

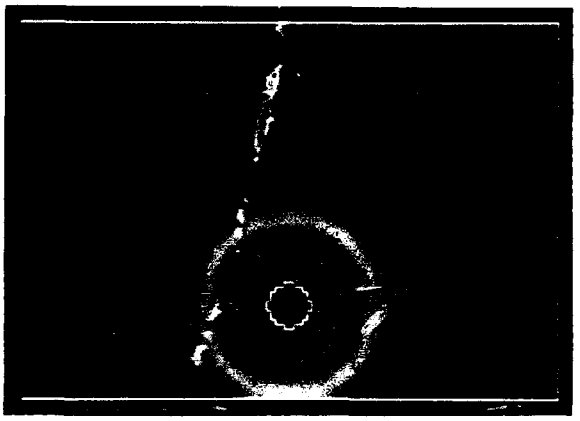

FIGURE 11. MASS DISTRIBUTION
(6.22E-05 SEC)

FIGURE 12. MASS DISTRIBUTION
(9.38E-05 SEC)

FIGURE 13. MASS DISTRIBUTION
(1.25E-04 SEC)

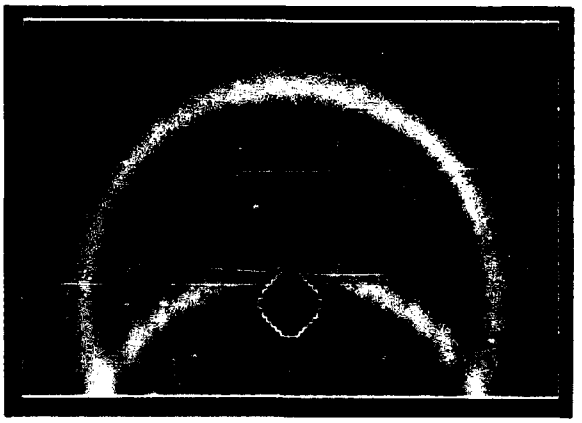

FIGURE 14. MASS DISTRIBUTION
(1.59E-04 SEC)

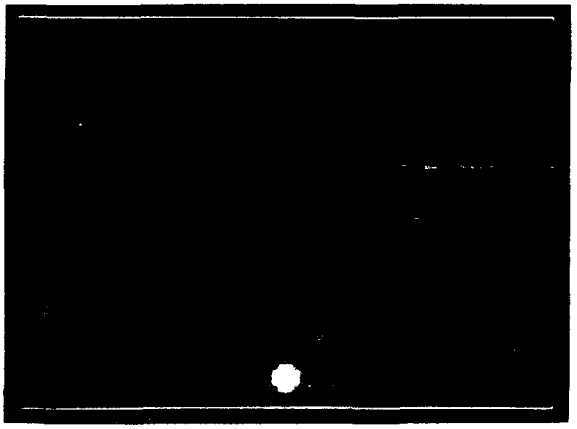

FIGURE 15. MASS DISTRIBUTION
(3.062E-04 SEC)

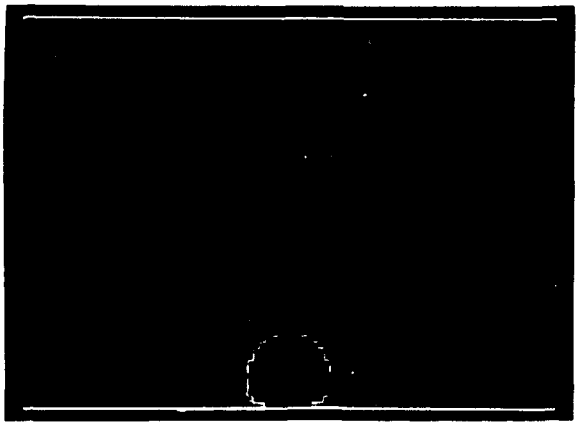

FIGURE 16. MASS DISTRIBUTION
(8.683E-03 SEC)

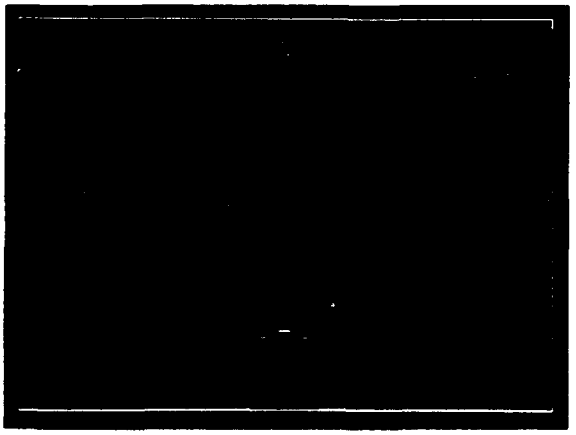

FIGURE 17. MASS DISTRIBUTION
(1.567E-02 SEC)

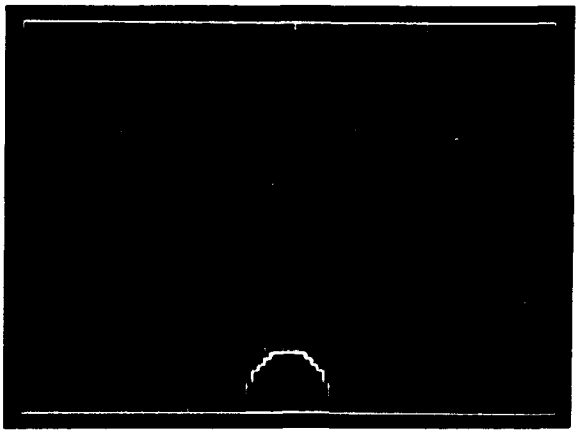

FIGURE 18. MASS DISTRIBUTION
(2.88E-02 SEC)

REFERENCES

1. Gentry, R. A., Martin, R. E., and Daly, B. J., "An Eulerian Differencing Method for Unsteady Compressible Flow Problems," J. Comp. Phys., Vol. 1, 1966 pp. 87-118.

2. Mader, C. L. Numerical Modeling of Detonations, University of California Press, Berkeley, CA, 1979.

3. Lee, E. L., and Tarver, C. M. "Phenomenological Model of Shock Initiation in Heterogeneous Explosives," Phys. Fluids, Vol. 23, No. 12, Dec. 1980, pp. 2362-2372.

4. Forest, C. A., Burning and Detonation, Los Alamos Scientific Laboratory, UC-45, La-7245, Jul 1978.

DISTRIBUTION

	Copies
Office of Naval Technology	
Attn: OCNR-20	1
OCNR-23	1
OCNR-232	1
OCNR-213	1
Ballston Center Towers #1, Rm 503	
800 No. Quincy Street	
Arlington, VA 22217-5000	
ODDR&E/Tactical Warfare	
Attn: R. Menz	1
The Pentagon	
Washington, DC 20301	
ODDR&E/Chief of Naval Operations	
Attn: OP-22	1
OP-225	1
OP-35	1
OP-353	1
OP-354	1
OP-374	1
OP-411	1
OP-71	1
OP-981	1
Technical Library	1
Department of the Navy	
Washington, DC 20350	
Commander	
Naval Sea Systems Command	
Attn: SEA-55X (D. Bruder)	1
SEA-55X (B. McCarthy)	1
SEA-402	1
SEA-406	1
SEA-407	1
SEA-423	1
Department of the Navy	
Washington, DC 20362	

	Copies
Commander	
David W. Taylor Research Center	
Attn: Code 17	1
Code 172	1
Code 175 (J. Sykes)	1
Code 175.1 (Dr. B. Whang)	1
Code 175.2 (W. Conley)	1
Code 175.2 (P. Manny)	1
Code 175.2 (D. Hagar)	1
Bethesda, MD 20084	
Office of Naval Research	
Attn: Code 1132-SM	1
Code 1132-P	1
Code 1132-F	1
Technical Library	1
800 North Quincy Street	
Arlington, VA 22217	
Director	
Defense Nuclear Agency	
Attn: Code SPSD (Dr. T. Tsai)	1
Code SPSD (Dr. K. Goering)	1
Code SPWE (C. McFarland)	1
Technical Library	1
Washington, DC 20305	
Lawrence Livermore National Laboratory	
Attn: B. Bowman	1
Technical Library	1
Livermore, CA 94550	
Director, Army Ballistics Research Laboratory	
Attn: Code IBD (S. Wilkerson)	5
Building 390	
Aberdeen Proving Ground, Maryland 21005	

DISTRIBUTION (Cont.)

	Copies
Library of Congress Attn: Gift & Exchange Division Washington, DC 20540	4
Defense Technical Information Center Cameron Station Alexandria, VA 22304-6145	12

Internal Distribution:		Copies
D4		1
E231		2
E232		3
H14		1
R		1
R10		1
R10A	(D. Phillips)	1
R10A	(K. W. Reed)	1
R11	(R. M. Doherty)	1
R14		1
R14	(F. Bandak)	1
R14	(R. Barash)	1
R14	(R. Bendt)	1
R14	(T. Farley)	1
R14	(J. Gaspin)	1
R14	(J. F. Goertner)	1
R14	(G. Harris)	1
R14	(Dr. H. Huang)	1
R14	(K. Kiddy)	1
R14	(J. Koenig)	1
R14	(D. Lehto)	1
R14	(H. Mair)	1
R14	(M. Mair)	1
R14	(W. McDonald)	1
R14	(M. Moussouros)	1
R14	(J. Shapiro)	1
R14	(G. Young)	1
R44	(W. Szymczak)	1
U		1
U02		1
U08		1
U11	(E. Johnson)	1
U12	(W. Hinckley)	1
U12	(C. Smith)	1
U12	(W. Walker)	1
U20		1
U24		1
U31	(Dr. C. McClure)	1